Annu. Rev. Phys. Chem. 1990. 41: 525–57

BLOCK COPOLYMER THERMODYNAMICS: Theory and Experiment

Frank S. Bates

Department of Chemical Engineering and Materials Science, University of Minnesota, Minneapolis, Minnesota 55455

Glenn H. Fredrickson[1]

AT&T Bell Laboratories, Murray Hill, New Jersey 07974

KEY WORDS: order and disorder.

INTRODUCTION

Block copolymers are macromolecules composed of sequences, or blocks, of chemically distinct repeat units. The development of this field originated with the discovery of termination-free anionic polymerization, which made possible the sequential addition of monomers to various carbanion-terminated ("living") linear polymer chains. Polymerization of just two distinct monomer types (e.g. styrene and isoprene) leads to a class of materials referred to as AB block copolymers. Within this class, a variety of molecular architectures is possible. For example, the simplest combination, obtained by the two-step anionic polymerization of A and B monomers, is an (A–B) dioblock copolymer. A three-step reaction provides for the preparation of (ABA) or (BAB) triblock copolymer. Alternatively, "living" diblock copolymers can be reacted with an n-functional coupling agent to produce $(A–B)_n$ star-block copolymers, where $n = 2$ constitutes a triblock copolymer. Several representative $(A–B)_n$ block copolymer architectures

[1] Present address: Department of Chemical and Nuclear Engineering, University of California, Santa Barbara, California 93106.

0066-426X/90/1101-0525$02.00

are illustrated in Figure 1. As a consequence of the "living" nature of these reactions, the resulting block and overall molecular weight distributions are nearly ideal, i.e. $M_W/M_N < 1.1$, where M_W and M_N represent the weight and number-average molecular weights, respectively.

Since the original studies of anionic block copolymerization in the 1950s (1, 2) a variety of new polymerization methods (e.g. condensation, Ziegler-Natta, etc.) have contributed to an expanding number of block copolymer classes (e.g. ABC) and novel architectures (e.g. graft-block). Although some of the developments have resulted in important new materials (e.g. polyurethanes), anionic polymerization remains the only viable method for

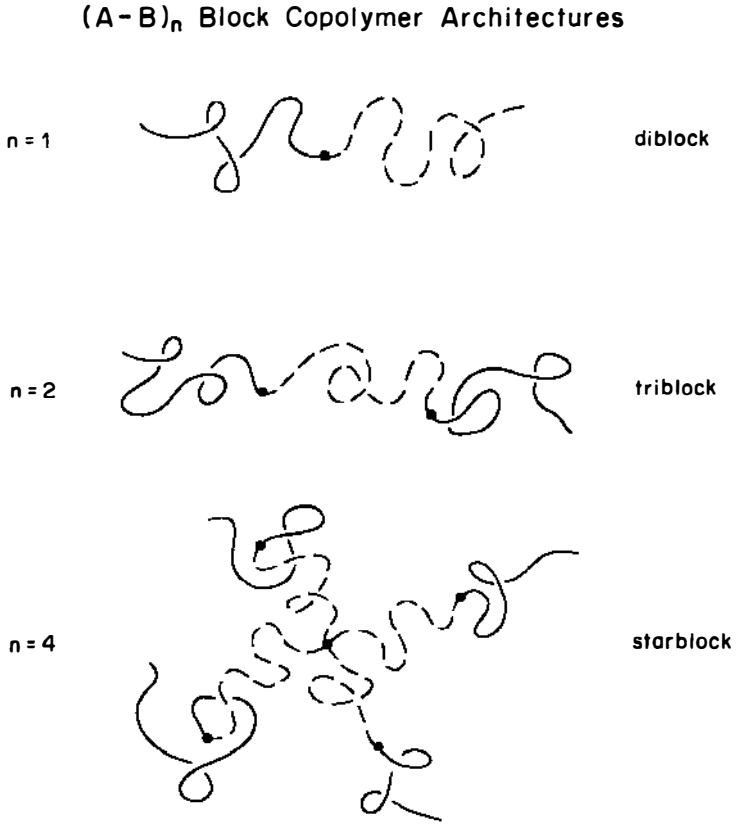

Figure 1 Schematic illustration of several $(A–B)_n$ type block copolymer architectures. *Solid* and *dashed lines* represent A and B block chains. The $n = 1$ and $n = 2$ architectures are commonly referred to as diblock and triblock copolymers, while $n \geq 3$ are denoted starblock copolymers.

producing monodisperse block copolymers with well-defined architectures. Because current theories deal almost exclusively with model $(A–B)_n$ type materials, we have restricted our attention in this review to studies based solely on this class of anionically polymerized block copolymers (see Figure 1).

The phase behavior of undiluted (bulk) $(A–B)_n$ block copolymers is determined by three experimentally controllable factors: the overall degree of polymerization N, architectural constraints characterized by n and the composition f (overall volume fraction of the A component), and the A–B segment-segment (Flory-Huggins) interaction parameter χ. [In the present review we use the terms monomer and segment interchangeably to imply statistical segment (3).] The first two factors are regulated through the polymerization stoichiometry and influence the translational and configurational entropy, whereas the magnitude of (the largely enthalpic) χ is determined by the selection of the A–B monomer pair. We note that for all the materials considered in this review, the interaction parameter has the temperature dependence $\chi \approx \alpha T^{-1} + \beta$, where $\alpha > 0$ and β are constants for given values of f and n. Since the $n = 1$ case has received the most comprehensive theoretical treatments and because the above factors qualitatively influence phase behavior independent of n, our introductory remarks and much of this text focus on diblock copolymers.

At equilibrium, a dense collection of monodisperse diblock copolymer chains will be arranged in minimum free energy configurations. Increasing the energy parameter χ (i.e. lowering the temperature) favors a reduction in A–B monomer contacts. If N is sufficiently large, this may be accomplished with some loss of translational and configurational entropy by local compositional ordering as illustrated in Figure 2 for the symmetric

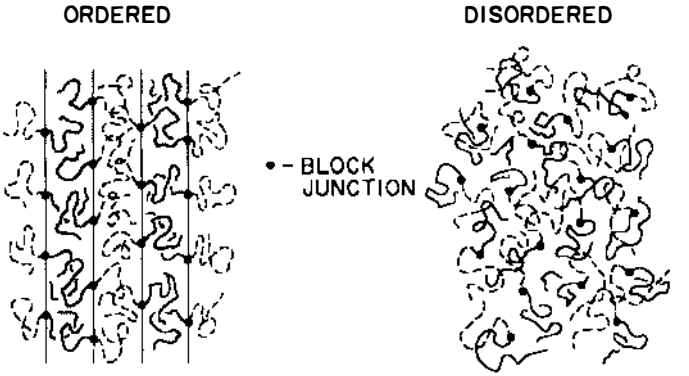

Figure 2 Schematic representation of order and disorder in a symmetric ($f = 1/2$) diblock copolymer showing lamellar order.

case $f = 0.5$. (Here we note that block crystallization, which can also occur, lies outside the scope of this paper; we consider only amorphous copolymers.) Such local segregation is often referred to as *microphase separation*; *macroscopic* phase separation is impossible in a single-component block copolymer. Alternatively, if either χ or N is decreased enough, the entropic factors will dominate, leading to a compositionally disordered phase. Since the entropic and enthalpic contributions to the free energy density scale as N^{-1} and χ, respectively, it is the product χN that dictates the block copolymer phase state. For $f = 0.5$, the transition between the ordered and disordered states occurs when $\chi N/n \sim 10$, as discussed below.

Two limiting regimes have been postulated to exist in the diblock copolymer phase diagram, as illustrated in Figure 3. For $\chi N \ll 1$, a copolymer melt is disordered and the A–B interactions sufficiently weak that the individual chain statistics are unperturbed (i.e. Gaussian). The connectivity of the two blocks and the incompressibility of the melt, however, lead to a correlation hole (3, 4) that is manifested in scattering measurements as a peak corresponding to a fluctuation length scale $D \sim R_g \sim aN^{1/2}$. (Here R_g is the copolymer radius of gyration and a is a characteristic segment length.) As χN is increased to be O(10), a delicate balance between energetic and entropic factors produces a disorder-to-order phase transition. It has been suggested that in the vicinity of this transition, the A–B interactions are sufficiently weak that the individual copolymers remain largely unper-

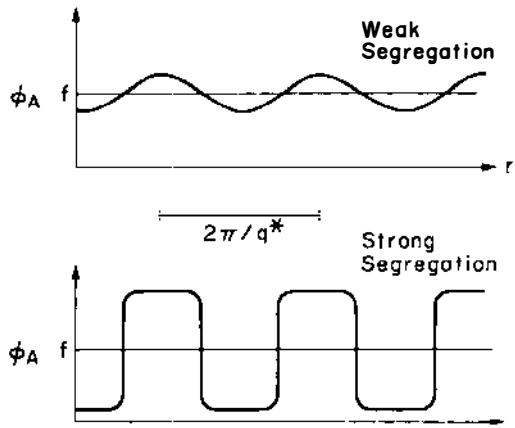

Figure 3 Comparison of the one-dimensional composition profiles characterizing the weak (WSL) and strong (SSL) segregation limits. ϕ_A and f refer to the local and stoichiometric (i.e. macroscopic) A-block volume fractions, respectively.

turbed, the microdomain period scales as $N^{1/2}$, and the ordered composition profile is approximately sinusoidal. We shall refer to such a regime as the *weak segregation limit* (WSL). Current order-disorder transition (ODT) theories are based on this WSL assumption because it greatly simplifies calculations, although strict adherence of experimental systems to the WSL postulates is still not established. The second limiting regime of phase behavior is referred to as the strong segregation limit (SSL) and corresponds to the situation of $\chi N \gg 10$. In this regime, narrow interfaces of width (5) $a\chi^{-1/2}$ separate well-developed, nearly pure A and B microdomains. The interaction energy associated with A–B contacts is localized in these interfacial regions; the system would like to minimize the total area of such interface, but must do so under the constraint of incompressibility and with the entropic penalty of extended chain configurations (5, 6). These opposing forces lead to perturbed chain configurations and microdomain dimensions (periods) that scale as $D \sim aN^{2/3}\chi^{1/6}$.

Since most theories and experiments dealing with block copolymer phase behavior can be categorized as either WSL or SSL, we have organized the present review under these general headings. As is discussed further below, this classification scheme may break down in the ODT region. Regardless, it proves most convenient to treat the transition region in the WSL section.

The preparation of model (undiluted) block copolymers for the purpose of studying the order-disorder transition (ODT) [also referred to as the microphase separation transition (MST)] is complicated by the limited range in χN afforded by experimentally accessible temperatures. In order to overcome this difficulty, researchers often add modest amounts of a neutral solvent to the bulk material, thereby diluting the A–B contacts. Here a neutral solvent is defined as one that shows no preference for either block type. In general, such concentrated solutions behave much like the bulk materials, with χ replaced by an effective interaction parameter that is proportional to the copolymer concentration. Thus, we have included this restricted group of block copolymer solution studies in the present review; semidilute and dilute copolymer solutions fall outside the scope of our review.

This review is organized into four sections, each dealing with theory and experiment. In the first and second sections we cover recent developments in the strong and weak segregation limits, respectively. Limitations in size constrain us to significant developments that have occurred within roughly the past decade. Prior advances in block copolymers are documented in earlier reviews (7–12). We further restrict ourselves to issues related to block copolymer thermodynamics, leaving a vast literature on copolymer dynamics to a future reviewer. In some instances, however, dynamical properties and measurements are inextricably coupled with thermo-

dynamic properties. In these circumstances we have not attempted to separate the issues. Our final topic, addressed in the third section, involves block copolymer surfaces. Recent experimental and theoretical advances in this emerging area have added a new dimension to the field of block copolymer thermodynamics. A discussion and outlook section is devoted to assessing recent progress in this field and to speculating on future directions.

STRONG SEGREGATION LIMIT (SSL)

Experiment

Until roughly a decade ago transmission electron microscopy (TEM) was the preeminent experimental technique for studying block copolymer structure. The combination of relatively large monodisperse microstructures and efficient heavy-metal staining techniques (e.g. osmium tetraoxide) produced truly spectacular electron micrographs of ordered phases in polystyrene-polydiene block copolymers. Five ordered phases were identified in the strong segregation limit. Two types of spherical and cylindrical microstructures, as well as a lamellar morphology (see Figure 4), were shown to exist within well-defined composition ranges in close agreement with Helfand's theoretical predictions (5). During the past decade, our analytical capabilities have been greatly enhanced by the development of small-angle scattering techniques that complement advances in TEM and provide access to new thermodynamic and fluctuation quantities. The topics covered in this section reflect these recent developments.

Hashimoto and co-workers have played a leading role in the application

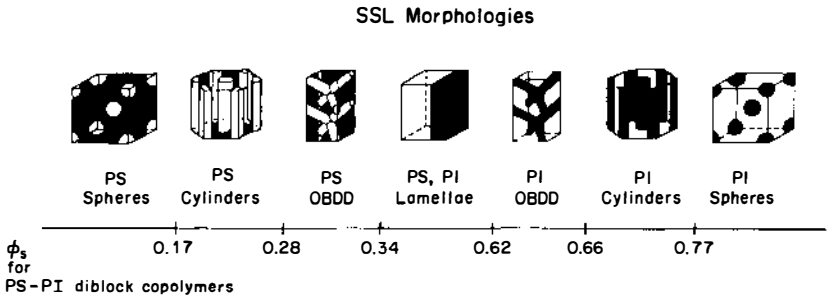

Figure 4 Strong segregation limit (SSL) equilibrium morphologies for $(A–B)_n$ type block copolymers. The order-order transition compositions shown apply to polystyrene-polyisoprene diblock copolymers where ϕ_s corresponds to the polystyrene volume fraction.

of small-angle X-ray scattering (SAXS) to the investigation of block copolymer thermodynamics. In a seminal series of publications (13–18) these authors used SAXS and TEM to explore microdomain size and packing, and interfacial mixing in a model set of polystyrene-polyisoprene diblock copolymers. The quantitative measurement of the interfacial thickness between microphases represented an important development, particularly in the light of theoretical predictions by Helfand & Wasserman (5) regarding this parameter. Following procedures developed by Ruland (19), Vonk (20), and others (21), Hashimoto et al evaluated the large scattering wavevector region of their SAXS data (the Porod regime) and determined an interfacial thickness $t = 20 \pm 5$ Å independent of microstructure (lamellar or spherical) and molecular weight. A subsequent SANS study of polystyrene-polybutadiene diblock copolymers by Bates et al (22) produced essentially the same conclusions regarding interfacial thickness. [These authors also determined body-centered-cubic packing of spherical polybutadiene domains (23) in agreement with the weak segregation prediction of Leibler (see WSL theory section). However, this packing symmetry may not be universal, since Richards & Thomason (24) have deduced a face-centered-cubic symmetry for polystyrene-polyisoprene diblock copolymers containing polystyrene spherical microdomains, also based on SANS measurements.] In independent SAXS measurements on polystyrene-polybutadiene diblock and triblock copolymers, Roe et al (25) found $10 \lesssim t \lesssim 17$ Å. [These authors report interfacial thickness measurements for $T > T_{ODT}$ (which we define as being in the WSL) suggesting the presence of microdomain structure within the disordered state.] All these small-angle scattering results for polystyrene-polydiene block copolymers are in reasonably good agreement with the prediction of Helfand & Wasserman (5), $t \approx \sqrt{2/3} a \chi^{-1/2} \cong 23$ Å (see SSL-Theory section), where a is the statistical segment length.

Although small-angle scattering experiments are capable of establishing a precise characteristic interfacial thickness, they are not able to discriminate between different mathematical expressions for the interfacial profiles due to limitations set by background and domain scattering. Spontak et al (26) have attempted to address this deficiency by measuring the interfacial composition profile directly via TEM. This method requires use of extremely thin osmium-stained sections, which raises questions regarding stain-induced local segregation and swelling. Nevertheless, Spontak et al report interfacial composition profiles with characteristic thicknesses, $t \approx 26$ Å, slightly greater than were found by the small-angle scattering Porod analysis.

One of the most exciting discoveries within the strong segregation regime in recent years is the ordered bicontinuous double diamond (OBDD)

morphology, depicted in Figure 4 along with the five originally recognized equilibrium morphologies. A representative electron micrograph of this morphology is shown in Figure 5. To our knowledge, the earliest published TEM picture of the OBDD phase was obtained from a polystyrene-polydiene star-block copolymer and reported by Aggarwal (27) as the "wagon wheel" morphology. Subsequently, Thomas and co-workers (28, 29) initiated a research program aimed at ellucidating the solid state morphology of well-defined star-block copolymers prepared by L. J. Fetters (30). For a narrow range of experimental conditions including arm number, molecular weight, and composition ($\approx$26% by volume polystyrene), Thomas et al found a novel bicontinuous morphology that did not conform to the well-known ordered phases. Soon thereafter came their dramatic identification of the now well-known OBDD phase (31), consisting of two continuous interpenetrating diamond (tetragonally coordinated) networks of polystyrene rods embedded in a continuous polyisoprene matrix. Evidence for this structure was provided by the combined use of SAXS and TEM. Small-angle scattering reflections from the ordered lattice were instrumental in identifying the exact lattice type and space group, which was then correlated with numerous tilted TEM images based on computer generated two-dimensional crystallographic projections.

Following these publications on star-block copolymers, Hasegawa et al (32) reported an equivalent ordered phase, denoted the "tetrapod-network structure" in polystyrene-polyisoprene diblock copolymers, thus demon-

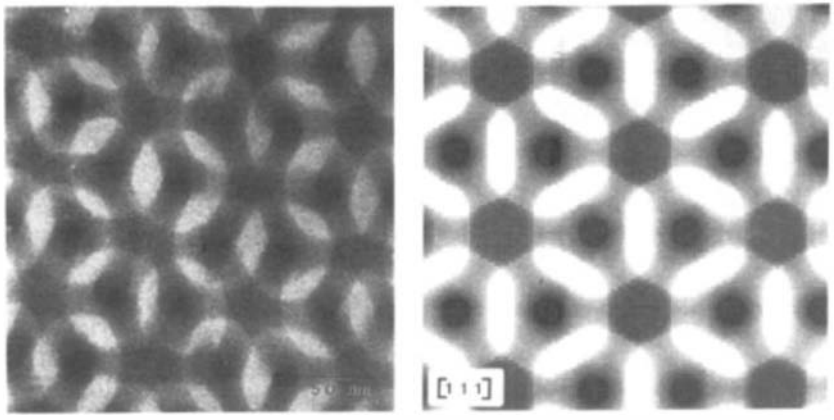

Figure 5 (*a*) Representative transmission electron micrograph of the ordered bicontinuous double diamond (OBDD) morphology. This image was obtained from an osmium stained polystyrene-polyisoprene block copolymer. (*b*) A computer simulated projection of the OBDD structure. (Provided by E. L. Thomas.)

strating the occurrence of the OBDD phase in simple linear block architectures. [Because these diblock copolymers contained polystyrene as the major component (62–66% by volume), the two interpenetrating networks were composed of polyisoprene, i.e. the "tetrapod-network structure" is actually an inverted version of the original OBDD phase identified by Thomas et al.] Both research groups evaluated the stability of this morphology by preferential solvent casting and annealing experiments. For a narrow range of compositions, which varies slightly with chain architecture, the OBDD phase appears to be the equilibrium state; for polystyrene-polyisoprene diblock copolymers this occurs for polystyrene volume fractions of 0.28–0.34 (polystyrene double diamond structure) and 0.62–0.66 (polyisoprene double diamond structure) as indicated in Figure 4 (32, 33).

Most recently, Thomas and co-workers have explored the underlying driving forces for the formation of the OBDD microstructure, demonstrating that it belongs to a class of geometrical structures characterized by constant mean curvature (CMC) surfaces (34). Several TEM images of new block copolymer morphologies were also presented and shown to belong to a family of periodic area-minimizing surfaces that have attracted the attention of mathematicians for over a century. These elegant studies have revealed a beautiful physical manifestation of abstract mathematical concepts, made possible through the careful control of the three molecular parameters described in the introduction.

Central to the theory of strong segregation in block copolymers is the concept of an extended block conformation, made necessary by the combined constraints of block joint localization at a narrow interface and an overall uniform density (see following section). The effects of extended chain conformation are most readily observed in the molecular weight dependence of the periodic lattice spacing and domain dimensions, $D \sim N^{\delta}$, where $\delta \approx 2/3$ in the SSL versus $\delta = 1/2$ for unperturbed chain statistics (assumed) in the WSL. With the advent of small-angle neutron scattering (SANS), the direct experimental determination of block chain statistics is now possible.

Richards & Thomason (35) reported the first SANS measurements on mixtures of partially labeled and unlabeled polystyrene-polyisoprene diblock copolymers. The SANS pattern contained two scattering contributions, one deriving from single-block scattering from within the polystyrene spherical domains (containing 4% deuterated polystyrene blocks) and a second associated with domain scattering. Richards & Thomason estimated the domain scattering contribution based on the SANS pattern obtained from an unlabeled sample, and subtracted it from the total scattering intensity to arrive at an estimate for the polystyrene block

dimensions within the spherical domains. Unfortunately, this subtraction method is extremely sensitive to small differences in molecular weight and composition between the labeled and unlabeled polymers, and this sensitivity limits the practical application of the method.

Hadziioannou et al (36) published the first SANS study of block chain dimensions in a lamellar microstructure. By mixing small amounts of partially deuterated polystyrene-polyisoprene block copolymer (per-deuterated polystyrene block) with equal molecular weight unlabeled material, these researchers created scattering contrast within the polystyrene domains that could be used to determine the average block conformation within the lamellae. As with the previous case, however, for the concentrations of labeled polymer used by Hadziioannou et al there is a strong scattering component due to interdomain interference that dominates the scattering intensity when the neutron beam is directed parallel to the plane of the lamellae. For unoriented (i.e. "polycrystalline") samples, this interference effect nearly completely obscures single block scattering. Hadziioannou et al partially rectified this problem by shear-orienting their material, thereby providing a purely perpendicular incident neutron beam geometry. This eliminates the interlamellar scattering component, and allows a direct determination of chain dimensions parallel to the lamellae. Perpendicular dimensions, however, could not be measured. Their study indicated a significant lateral contraction of the block chain dimensions parallel to the lamellae, relative to the unconstrained size.

The topic of single chain scattering in undiluted block copolymers was treated theoretically by Jahshan & Summerfield (37) and Koberstein (38) in the early 1980s. These authors recognized that by mixing specified amounts of partially labeled and unlabeled chains, the contrast factor (i.e. the scattering length density for neutrons) could be matched between microphases, thus eliminating domain scattering. Within a microdomain, however, isotopic labeling would give rise to single block scattering. This contrast matching technique was first demonstrated by Bates et al (39) in a polystyrene-polybutadiene diblock copolymer system in which spherical microdomains were prepared with 16% perdeuterated and 84% hydrogenous polybutadiene blocks. The method proved to be quite effective at eliminating domain scattering, and for low molecular weight polybutadiene blocks revealed an overall radius of gyration in agreement with unperturbed dimensions. However, as the molecular weight was increased, the apparent block dimensions became unreasonably large; this behavior can now be attributed to small deviations from the exact contrast matching condition or to fluctuation effects (see below).

The most recent studies of block chain statistics have made use of the contrast matching technique with the lamellar morphology. This com-

bination affords acccss to both the lateral (parallel) and perpendicular components of the chain conformation within the microdomain space. SANS studies by Hasegawa et al (40, 41) and Matsushita et al (42) demonstrate that even at the theoretical contrast matching condition, some residual domain scattering remains due to slight composition fluctuations within the isotopically mixed microphase; increasing molecular weight exacerbated this problem, as inadvertently found by Bates et al (39). Nevertheless, contrast matching reduces the interference effects by up to two orders of magnitude, thereby facilitating the determination of the perpendicular block dimension. Hasegawa et al (40, 41) report polystyrene block chain dimensions parallel and perpendicular to the lamellae to be approximately 70% and 160% of the unperturbed dimensions, respectively, for nearly symmetric polystyrene-polyisoprene diblock copolymers when $M_w = (7.5-10) \times 10^4$ g/mole.

Theory

By the middle of the 1970s, thc physical principles that govern the microdomain period and the selection of ordered phases in the SSL had been well-established by pioneering studies of Meier (43), Leary & Williams (44), and Helfand & Wasserman (5, 45a,b). Most notably, Helfand & Wasserman developed a self-consistent field theory that permits quantitative calculations of free energies, composition profiles, and chain conformations. They identified the three principal contributions to the free energy in the regime $\chi N \gg 10$ as arising from (*a*) contact enthalpy in the narrow interfaces between nearly pure A and B microdomains, (*b*) entropy loss associated with extended chain configurations to ensure incompressibility (i.e. stretching free energy), and (*c*) confinement entropy due to localization of the block copolymer joints (covalent bonding sites between blocks) to the interfacial regions. Helfand & Wasserman showed that these narrow interfaces have characteristic thickness $a\chi^{-1/2}$, and by *numerical* solutions of the self-consistent field equations proposed that the microdomain period scales (asymptotically for $N \to \infty$) as $D \sim aN^{\delta}\chi^{\mu}$, with $\delta \approx 9/14 \approx 0.643$ and $\mu \approx 1/7 \approx 0.143$. In this asymptotic limit the confinement entropy of the junction is negligible compared with the stretching entropy. Helfand & Wasserman also developed numerical techniques for calculating the phase diagram in the SSL, and located the (virtually temperature independent) compositions that delimit the thermodynamic stability of spheres, cylinders, and lamellae. These compositions are in good agreement with experimental determinations of the phasc boundaries, although we note that the OBDD phase (having not yet been discovered) was not included in the free energy competition.

Although the Helfand-Wasserman theory is believed to contain all the

proper physical ingredients necessary to describe the SSL, its practical application has been hindered because of the requirement of rather difficult numerical analysis. The theoretical advances of the past decade have been focused on developing *analytical* methods for estimating the free energy in the asymptotic limit $\chi N \to \infty$. Probably the most influential of these modern studies was a paper by Semenov (6), which addressed a diblock melt in the SSL. Semenov argued that because the copolymers are strongly stretched in this regime (see previous section), the required configurational integrals are dominated by the classical extremum of the energy functional (Hamiltonian). The extremum path corresponds to the most probable configuration of a copolymer block as it extends from an interface into a microdomain and experiences the chemical potential field produced by the surrounding molecules. Moreover, Semenov showed that the differential equation describing this path (which resembles the equation of motion of a classical particle) is analytically soluble, even when the chemical potential is determined self-consistently to maintain constant density of copolymer segments. This solution indicates that the copolymers are stretched nonuniformly (along their contours) as they enter into the microdomains and predicts that the chain ends are distributed at excess in the domain interiors. The classical mechanical analogy identified by Semenov has been further clarified by Milner, Witten & Cates (46, 47a,b) and was extensively exploited by these authors to treat related problems of grafted polymer brushes and surfactant interfaces. To appreciate the reduction in complexity afforded by this method, we note that the Helfand-Wasserman approach corresponds to the solution of a time-dependent problem in quantum mechanics, whereas the Semenov-Milner-Witten-Cates approach requires only the solution to the classical limit of this problem. Of course, the latter approach is only legitimate under conditions of strong chain stretching.

It is somewhat surprising that in spite of the significant chain deformations predicted for the SSL, the domain (stretching) contribution to the free energy per chain was found by Semenov to have the same scaling as for a Gaussian chain, namely $F_{\text{domain}}/kT \sim D^2/a^2N$, where D is the domain period. It is only the constant prefactor omitted from this expression that reflects the nonuniform stretching and distribution of ends. In the asymptotic limit $\chi N \to \infty$, the domain free energy is balanced by the interfacial energy, which (per chain) is given by (5, 6, 45a,b) $F_{\text{interface}}/kT \sim \gamma\sigma \sim Na\chi^{1/2}/D$. Here we have inserted well-known results for the interfacial tension, $\gamma \sim \chi^{1/2}a^{-2}$, and for the area per chain, $\sigma \sim Na^3/D$. By balancing the two free energy contributions, Semenov's prediction for the domain period is recovered, $D \sim aN^{2/3}\chi^{1/6}$. This result is believed to be asymptotically correct for large incompatibility, as the fluctuations about

the classical path are $O(N^{1/2})$ and thus can be neglected for $N \to \infty$. The slight differences of these exponents from those of Helfand & Wasserman can be traced to the Helfand-Wasserman numerical estimate of F_{domain}. In particular, these authors found $F_{\text{domain}}/kT \sim (D/aN^{1/2})^{2.5}$, based on numerical calculations that extended only to $D/aN^{1/2} \approx 3$. We suspect that if the numerics had been carried out to $D/aN^{1/2} \gg 1$, the asymptotic scaling of Semenov would have been obtained. Finally, we note that Semenov's theory also provides estimates of the compositions that delimit the various ordered phases. As with the Helfand-Wasserman theory, these compositions are predicted to be temperature-independent.

Another notable SSL theory of the past decade is that due to Ohta & Kawasaki (48a,b). Like the Helfand-Wasserman and Semenov theories, the approach of Ohta & Kawasaki was field-theoretic, although Ohta & Kawasaki employed only a single scalar field describing the composition patterns. As a result, the physics associated with a nonuniform placement of chain ends is lost in this approach. Moreover, Ohta & Kawasaki used a random phase approximation for the free energy functional that is rigorously valid only for very weak compositional inhomogeneities, even though the inhomogeneities that characterize the SSL are O(1) in volume fraction. In spite of this, Ohta & Kawasaki were able to obtain predictions for the domain periods and phase diagram that are qualitatively similar to those of Helfand-Wasserman and Semenov. They have also been able to reduce the calculation of the microdomain free energies to a purely geometrical problem.

Finally, we mention the SSL theory of Anderson & Thomas (49), which is the only theory thus far to contend with the OBDD phase. These authors modified the Ohta-Kawasaki approach to treat $(A–B)_n$ star block copolymers. Although they found good agreement of the theoretical OBDD lattice parameters with experiment, Anderson & Thomas were not able to predict thermodynamic stability of the OBDD phase in the composition window where it is experimentally observed. Treatment of the OBDD phase with the methods of Helfand-Wasserman or Semenov has yet to be carried out.

WEAK SEGREGATION LIMIT (WSL)

Theory

Whereas the theoretical advances in the SSL were catalyzed by pioneering experiments involving the synthesis and characterization of model copolymers, developments in the WSL were strongly influenced by a seminal theoretical paper by Leibler (4). Leibler considered the case of a monodisperse A–B diblock copolymer melt with degree of polymerization N,

composition f, and equal monomer volumes and statistical segment lengths. For such a system, Leibler constructed a Landau expansion of the free energy to fourth order in a compositional order parameter field, $\psi(\mathbf{r}) = \langle \delta\phi_A(\mathbf{r}) \rangle$, where $\delta\phi_A(\mathbf{r}) = \phi_A(\mathbf{r}) - f$ is the fluctuation in microscopic volume fraction of A monomers at position $\mathbf{r}$. Such expansions prove useful in the vicinity of a second-order or weak first-order phase transition, where the amplitude of the order parameter field remains small in the low temperature phase (50). Indeed, the ODT of symmetric ($f = 0.5$) or weakly asymmetric block copolymers is such a transition. Leibler's calculation was particularly remarkable, because he provided microscopic expressions for the (Landau) expansion coefficients as functions of the incompatibility, χN, and the copolymer composition. These coefficients were computed by means of the random phase approximation, introduced for polymer melt applications by de Gennes (3, 51).

By retaining only the leading harmonics in a Fourier representation of the various ordered-phase composition patterns, Leibler was able to exploit the Landau expansion and map out the phase diagram of a diblock copolymer melt near the ODT. (This approximation of neglecting higher harmonics in the description of the composition patterns can be rigorously justified only for the case of a second-order phase transition, but is expected to remain quantitative in weak first-order situations. Note also that the OBDD phase was not explicitly included in the free energy competition.) The phase diagram so obtained, in the parameter space of χN and f, is shown in Figure 6*a*. The Landau theory predicts a critical point at $(\chi N)_c = 10.5, f_c = 0.5$, where a compositionally symmetric diblock melt is expected to undergo a second-order phase transition from the disordered to the lamellar phase. At such a transition, the amplitude of the lamellar pattern grows continuously from zero on lowering the temperature (i.e. increasing χN). The lattice constant (period) of the lamellar phase is predicted to be $D \approx 3.23 R_g \sim N^{1/2}$ at the symmetric ODT, consistent with the WSL assumption that the copolymers are only weakly perturbed by the inhomogeneous composition field. For asymmetric diblock copolymers, $f \neq 0.5$, the Landau theory predicts a weak first-order transition from the disordered phase to the BCC spherical phase. In contrast to the situation in the SSL, it is important to note that the Landau theory predicts first-order transitions between solid phases that can be accessed by changing temperature.

Besides the phase diagram shown in Figure 6*a*, Leibler (4) provided an expression for the disordered phase structure factor, $S(q) = \langle \delta\phi_A(\mathbf{q}) \delta\phi_A(-\mathbf{q}) \rangle$, given by

$$S^{-1}(q) = N^{-1} F(x,f) - 2\chi \qquad 1.$$

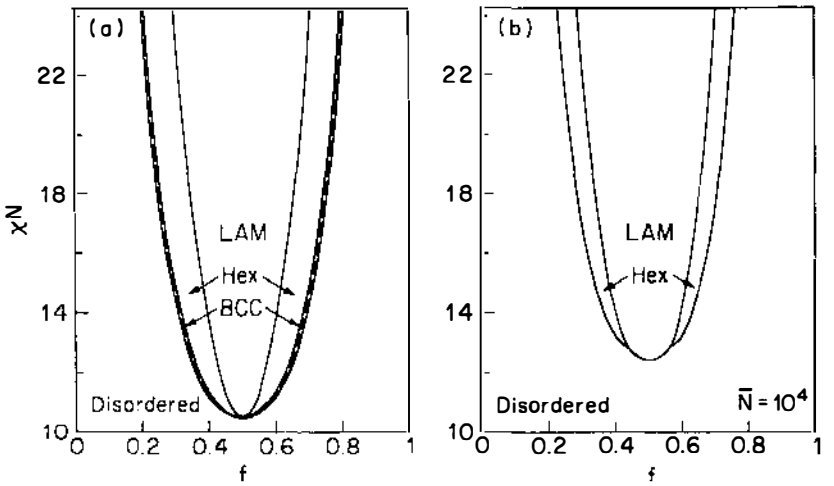

Figure 6 Theoretical phase diagrams for diblock copolymers in the weak segregation limit: (*a*) mean-field theory (4); (*b*) fluctuation theory with $\bar{N} = 10^4$ (62). LAM, Hex, and BCC correspond to lamellar, hexagonal (cylindrical morphology), and body-centered-cubic (spherical morphology) symmetries, and the *dashed curve* represents the mean-field (Landau) stability limit. (Reproduced from Ref. 63.)

where $x \equiv q^2R_g^2$ and $F(x,f)$ is a dimensionless function of wavenumber and composition that is related to certain (Debye) correlation functions of a Gaussian diblock copolymer (4). The most characteristic feature of this expression is the prediction of a Lorentzian peak at $x = x^*(f) \sim O(1)$, where F is minimum; the peak intensity diverges at the classical spinodal given by the condition $F(x^*,f) - 2(\chi N)_s = 0$. In the Landau theory, the spinodal and critical point coincide for $f = 0.5$. It should be noted that expressions similar to Eq. 1 were also derived by LeGrand & LeGrand (52) and by de Gennes (51).

The above expression for $S(q)$ has facilitated the interpretation of numerous X-ray and neutron scattering measurements on partially labeled model diblock copolymers. Similar expressions for more complex block copolymer architectures, such as graft and star copolymers, have been derived by Olvera de la Cruz & Sanchez (53) and by Benoit & Hadziioannou (54). Other workers (55–58) have extended the Leibler expression to incorporate polydispersity effects, which are often important in practical applications. The latter extension is generally performed by averaging the Debye correlation functions that constitute $F(x,f)$ with an appropriate molecular weight distribution function, e.g. the Schultz-Zimm function.

It was recognized by Leibler (4) that the Landau theory, which predicts mean-field critical behavior (59), is inadequate in the vicinity of the $f = 0.5$ critical point discussed above. Brazovskii (60) had previously demonstrated that such critical points, predicted by mean-field theories for systems exhibiting transitions between isotropic and striped (i.e. lamellar) phases, are suppressed by large-amplitude order parameter fluctuations. By means of a self-consistent Hartree approximation, Brazovskii showed that the mean-field critical point is replaced by a weak first-order phase transition, induced by fluctuations. It should be emphasized that such *fluctuation-induced first-order phase transitions* (61) have been predicted to occur in a variety of other physical systems, such as liquid crystals and driven (nonequilibrium) fluids. Experiments to test these predictions, however, have been quite limited.

Fredrickson & Helfand (62) extended Brazovskii's Hartree method of analysis to the A–B diblock copolymer melt considered by Leibler. They found that the fluctuation corrections are controlled by a Ginzburg parameter (59) $\bar{N}$, proportional to the copolymer molecular weight, defined by $\bar{N} = 6^3(R_g^3\rho_c)^2$, where ρ_c is the number density of copolymers in the melt. For fixed incompatibility χN, but $\bar{N} \to \infty$, Fredrickson & Helfand found that Leibler's mean-field predictions are asymptotically approached. For finitc $\bar{N}$, however, the fluctuation corrections impose both qualitative and quantitative changes in the phase diagram (Figure 6*b*) and scattering behavior. In particular, the Hartree approximation leads to a suppression of the symmetric critical point at $(\chi N)_c = 10.5$, which is replaced by a weak first-order transition at (a lower temperature) $(\chi N)_{ODT} = 10.5 + 41.0\bar{N}^{-1/3}$. The amplitude of the lamellar composition pattern is predicted to be $O(\bar{N}^{-1/6})$ at the ODT. Because $\bar{N}$ is of order 10^3–10^4 for the typical experimental sample, these fluctuation corrections can be substantial. The changes in the phase diagram for asymmetric diblocks are even more dramatic, as is indicated in Figure 6*b* for $\bar{N} = 10^4$. An important distinction with the mean-field diagram 6*a* is that the lamellar and the hexagonal phases are accessible at the ODT in the Hartree approximation for $f \neq 0.5$. However, the mean-field prediction of first-order transitions between ordered phases that can be accessed by changing temperature is preserved in the Hartree approximation.

The fluctuations manifest in the Fredrickson-Helfand theory also impact the structure factor of the disordered and ordered phases. For the disordered phase, the Hartree approximation for $S(q)$ has the same wavenumber dependence as in Eq. 1, but the bare Flory parameter χ is renormalized by composition fluctuations to an effective interaction parameter χ_{eff}. This renormalized parameter depends on temperature, composition, and molecular weight and is related to the bare parameter by

$$\chi_{\text{eff}}N = \chi N - \frac{C(f)}{2N^{1/2}}[F(x^*,f) - 2\chi_{\text{eff}}N]^{1/2} \qquad 2.$$

where $C(f)$ is a composition-dependent coefficient. For a symmetric melt, the peak intensity $S(q^*)$ attains a maximum value that is $O(N\bar{N}^{1/3})$ at the ODT. In contrast, the mean-field theory gives rise to a divergent peak intensity at the symmetric ODT. The Hartree approximation also predicts an isotropic scattering component (in addition to the Bragg peaks) for the weakly ordered phases (62, 63). This fluctuation component is also $O(N\bar{N}^{1/3})$, but is lower in intensity than the pretransitional disordered-phase component.

The Hartree approximation leads to an interesting physical picture of a symmetric diblock copolymer melt in the vicinity of the ODT (63). Whereas the Landau theory gives statistical weight only to the extremum composition field configurations in the ordered and disordered phases, namely the uniform and perfectly ordered configurations shown in Figure 7*a*, the Hartree approximation also weights configurations like those shown in Figure 7*b*. The latter configurations have superimposed upon the extremum configurations isotropic composition fluctuations that have a preferred wavelength, $2\pi/q^*$, but random directions and phases. The Fredrickson-Helfand theory (62) suggests that the root-mean-squared amplitude of these fluctuations is $O(\bar{N}^{-1/6})$ and is thus comparable to the amplitude of the long-range-ordered lamellar component. It is interesting to note that the typical *equilibrium* composition field configurations in a disordered diblock melt (which fluctuate in time) are reminiscent of the transient *nonequilibrium* patterns encountered during the intermediate and late stages of spinodal decomposition (64).

A recent theoretical study of Semenov (65) suggests that the asymmetric wings of the phase diagram, i.e. $f \ll 0.5$ and $1-f \ll 0.5$, could be much more complicated than is predicted by the Landau or Hartree theories. By using techniques discussed above for the SSL (6), Semenov argues that the free energy of formation of spherical micelles changes sign at an incompatibility $(\chi N)_M$ that is lower than the Landau or Hartree $(\chi N)_{ODT}$. Such micelles are localized, large amplitude fluctuations in an (otherwise disordered) asymmetric diblock copolymer melt that are not accessible by the perturbative WSL approach described in the present section. Due to the favorable energetics of micelle formation near $(\chi N)_M$, Semenov postulates the existence of a spherical micellar phase that becomes more concentrated in micelles as χN is increased. By computing the interaction energy between two micelles, he further predicts a phase transition at which the micelles order into a macrolattice with fcc symmetry. If Semenov's arguments are correct, this transition constitutes the ODT for asymmetric

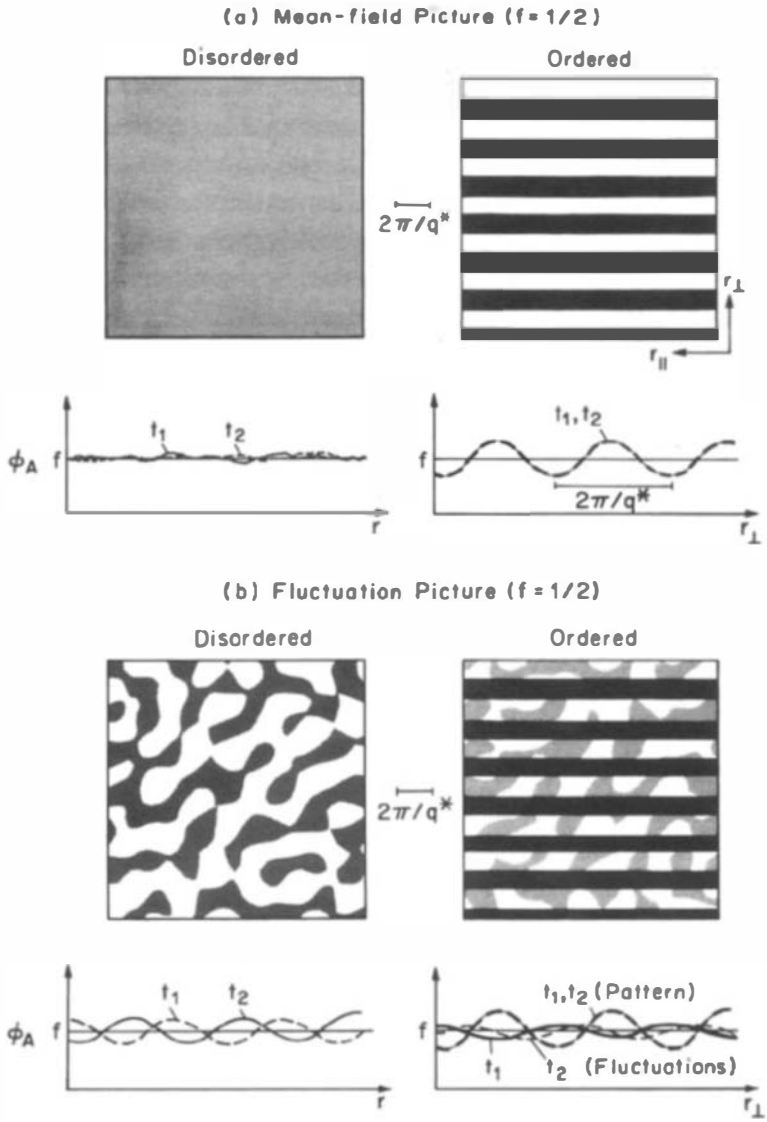

Figure 7 Instantaneous real-space composition patterns in the weak segregation limit: (*a*) mean-field theory, and (*b*) fluctuation theory. ϕ_A versus r depicts the expected time dependence ($t_1 \neq t_2$) of each morphology, where ϕ_A is the local volume fraction of A segments. Recent SANS results support the fluctuation picture near the order-disorder transition (see Figure 8). (Reproduced from Ref. 63.)

copolymers. Subsequent first order structural transitions into hexagonal and bcc phases are also predicted by the theory.

At the time of this writing, the Hartree approximation has been explored for triblock copolymers (66) but not for more complex block copolymer architectures, such as stars. However, the extension to concentrated and semidilute diblock copolymer solutions with a neutral (nonselective) solvent has recently been carried out (67, 68). It has frequently been assumed (69) that copolymer solutions have a uniform distribution of the nonselective solvent in the ordered microphases. This suggests that in the concentrated regime, where swelling effects are absent, the phase diagram of a copolymer solution is simply obtained by rescaling χ to $\phi\chi$ in the melt phase diagram, where ϕ is the copolymer volume fraction. Fredrickson & Leibler (67) have shown that this "dilution approximation" method (69, 70) neglects several aspects of the physics of such solutions. In particular, these authors demonstrated that even in the WSL there is a tendency for a neutral, good solvent to accumulate at the interfaces of the microdomains. This nonuniform placement of the solvent screens the unfavorable A–B monomer contacts, but does so with a translational entropy price. Screening occurs until that entropy cost exactly compensates the loss of contact enthalpy. For a good solvent, this compensation produces a periodic solvent composition profile with an amplitude that is N^{-1} smaller than the amplitude of the A–B composition profile. As the solvent quality is decreased, the two order parameter fields have comparable amplitudes in the weakly-ordered microphases and a tricritical point is encountered (67). Another aspect of neutral copolymer solutions that distinguishes them from molten copolymers, is that the ODT is associated with a two-phase region in which disordered solvent-rich and ordered solvent-poor phases coexist. This region is very narrow for good solvents, but broadens as the solvent quality is decreased. Finally, we note that by reformulating the melt Hartree approximation in terms of concentration blobs, the important case of semidilute neutral copolymer solutions can be treated (67, 68).

Experiment

As discussed in the previous section, bulk block copolymers can be brought into the weak segregation regime by decreasing either χ or N. The former is generally accomplished by selecting structurally similar monomers. For example, block copolymers ($f \sim 1/2$) prepared from styrene and α-methylstyrene remain disordered (i.e. homogeneous) at around 180°C for $M_w \lesssim 5 \cdot 10^5$ g/mole (71–73). In contrast, symmetric polystyrene-polydiene block copolymers exhibit an order-disorder transition at about this temperature when $10^4 \lesssim M_w \lesssim 2 \cdot 10^4$ g/mole, depending upon the polydiene type (e.g.

polybutadiene or polyisoprene) and microstructure (74, 75). Since these first reported, and in practice limiting cases, only a handful of block copolymers have been investigated in the WSL.

Pioneering studies by Cohen and co-workers (76, 78) on polydiene-polydiene diblock copolymers were conducted at about the time that the first WSL theory was developed. These investigations demonstrated WSL behavior in 1,4-polyisoprene-1,4-polybutadiene (76, 77) and 1,4-polybutadiene-1,2-polybutadiene (78) block copolymers that qualitatively supported Leibler's mean-field predictions, and gave impetus for subsequent research based on this class of materials. Since then, WSL investigations have been conducted with hydrogenated polystyrene-polydiene (75), polystyrene-poly(para-methylstyrene) (79), poly(ethylene-propylene)-poly(ethylethylene) (63, 80–82), and polystyrene-polymethylmethacrylate (57, 83, 84) block copolymers. In addition, modest amounts of neutral solvents ($\lesssim 60\%$) have been added to polystyrene-polydiene materials in order to decrease the order-disorder transition-temperature, thus bringing the WSL into the experimentally accessible temperature range (69, 85–87).

Within the weak segregation regime the most significant feature is the order-disorder transition. Identification of the ODT temperature, denoted T_{ODT}, is often complicated by the weak first-order character of this phase transition and the presence of significant composition fluctuations above and below T_{ODT}. Earlier studies established phase behavior based on the calorimetric or dynamic mechanical evaluation of the glass transition; a single glass transition is indicative of homogeneity (i.e. disorder), whereas two glass transitions signal microphase separation (i.e. order) (71–73, 75–78). Although these techniques remain useful screening methods (80, 88), they are incapable of quantitatively establishing T_{ODT}.

The ordering of a block copolymer is accompanied by gross changes in the low frequency rheological properties as first shown by Chung et al (89a,b), and Pico & Williams (90) for a poly(styrene-butadiene-styrene) (SBS) triblock copolymer, and plasticized SBS, respectively. This behavior is characterized by the transition from a terminal dynamic mechanical response for $T > T_{ODT}$ [e.g. $G' \sim \omega^2$ and $G'' \sim \omega$ for $\omega \to 0$ where G' and G'' are the dynamic elastic and loss moduli (91), respectively] to a non-terminal response for $T < T_{ODT}$. At sufficiently low frequencies, G', and to a lesser extent G'', drop discontinuously as the temperature is raised through the first-order ODT. This discontinuity provides a quantitative means of identifying T_{ODT}; typical rheometer temperature control affords approximately 1°C precision in the determination of T_{ODT}. This technique has been demonstrated and exploited by several research groups studying both diblock (82, 92) and triblock (93–97) copolymers, and in our judgement represents the most efficient and accurate method for establishing T_{ODT}.

In addition to these abrupt changes in the limiting low frequency ($\omega \to 0$) rheological properties at the ODT, composition fluctuations near the phase transition (see Figure 7) lead to significant departures from thermorheological simplicity (82, 92). A complete discussion of this dynamical behavior falls outside the scope of this review of block copolymer thermodynamics. Nevertheless, the continuous development of thermorheological complexity, particularly in the disordered state, is a direct manifestation of the fluctuation (i.e. thermodynamic) effects discussed previously and described below, and should not be confused with the discontinuous changes that mark the ODT (93).

As with the strong segregation limit, SAXS and SANS are very powerful and important experimental tools for investigating block copolymers in the weak segregation limit. The choice of X-rays or neutrons as incident radiation is dictated primarily by the choice of polymers, which determine the contrast factor. Nonpolar systems governed by relatively large χ parameters such as polystyrene-polydiene generally exhibit a sizeable electron density difference between components, which provides good X-ray contrast. Accordingly, these materials are frequently studied by SAXS. Increasing block compatability by selecting structurally similar polymers such as isomers (78, 88) greatly reduces or eliminates X-ray contrast, making the use of SAXS either difficult or impossible. In this situation, deuterium labeling (e.g. deuterating one block) provides strong neutron contrast, thus making SANS the experimental method of choice. These considerations are particularly important in the WSL. An intrinsically weak contrast factor [i.e. similar pure component electron (for SAXS) or neutron scattering length (for SANS) densities] will be sensitive to small changes in the local specific volume. Therefore, any inhomogeneously distributed (i.e. composition dependent) excess volume of mixing will modify this factor. If the local composition pattern changes with temperature, the contrast factor will vary with temperature. This effect will be most severe when the composition profile is most temperature dependent, i.e. near the ODT. Such a spurious temperature dependence to the scattering intensity would preclude the quantitative evaluation of theory.

Shortly after publication of Leibler's landmark WSL theory, Roe et al (25) demonstrated the existence of a broad temperature dependent SAXS peak in a polystyrene-polybutadiene diblock copolymer above T_{ODT}. This, and other similar experiments (69), were found to be qualitatively consistent with Eq. 1, i.e. decreasing temperature in the disordered state led to an increase in the peak scattering intensity. Quantitative assessments of Eq. 1 were first reported by Bates (56, 98) based on SANS measurements on partially deuterated 1,4-polybutadiene-1,2-polybutadiene (1,4PB-1,2PB)

diblock copolymers and by Mori et al (74), who studied polystyrene-polyisoprene (PS-PI) diblock copolymers by SAXS. These investigations demonstrated consistency between the measured and predicted disordered state structure factor for $f \sim 1/2$, and for the first time provided estimates of $\chi(T)$ obtained by fitting Eq. 1 to temperature dependent small angle scattering data, as originally proposed by Leibler (4). Although the scattering results for the symmetric diblock copolymers produced results that were in good agreement with theory, Bates & Hartney (56) found a significant discrepancy between Eq. 1 and SANS data obtained from a series of asymmetric ($f \cong 0.25$) disordered 1,4PB-1,2PB samples. Along with the expected scattering peak at wavevector q^* these materials produced a significant forward scattering component that increased in intensity with increasing N. Bates & Hartney (56) speculated that this feature could derive from (domain-like) entities present in the disordered melt. The recent prediction by Semenov (65) regarding micelle formation in the disordered state (see previous section) is consistent with these observations. These measurements have not been confirmed, however, and the issue of micelle formation in the disordered state remains unresolved.

As discussed in the previous section, Fredrickson & Helfand (62) have recently incorporated fluctuation effects into Leibler's original weak segregation mean-field theory, arriving at the phase diagram illustrated in Figure 6 ($\bar{N} = 10^4$). Several experimentally testable differences between the mean-field and fluctuation theories can be identified. As the ODT is approached in the disordered phase, both theories anticipate a rapid increase in the peak scattering intensity $I(q^*) \sim S(q^*)$ as indicated by Eq. 1. However, for the general case in which $\chi = \alpha T^{-1} + \beta$ (see Introduction) the mean-field and fluctuation theories differ significantly in the predicted temperature dependence of $I(q^*)$; the former predicts $I^{-1}(q^*)$ to be linear in T^{-1}, whereas fluctuation effects produce a nonlinear relationship between these parameters (see Eq. 2).

Beginning with Roe and co-workers (25), the order-disorder transition has been examined in a variety of polystyrene-polydiene diblock (25, 76, 86), triblock (95), and star-block (86, 87) copolymers and hydrogenated polystyrene-polybutadiene diblock copolymers (75) by small-angle X-ray scattering. These studies have relied on SAXS data obtained as a function of temperature for determining T_{ODT}. In general, the ODT has been correlated with the temperature when a deviation from lincarity in a plot of $I^{-1}(q^*)$ versus T^{-1} is observed, which assumes mean-field behavior (25, 75, 95). Alternatively, Hashimoto et al (86, 87) have relied on the temperature dependence of the scattering peak position q^* in fixing T_{ODT}. [Previously these authors reported $q^* \sim T^0$ for $T > T_{ODT}$ and $q^* \sim T^{1/3}$ for $T < T_{ODT}$ (69). Neglecting the intrinsic polymer coil thermal expansivity, the WSL

and SSL theories predict $q^* \sim T^0$ and $q^* \sim T^{1/6}$, respectively (see Theory sections).] In all these SAXS studies the ODT appears as a continuous transition as evidenced by an unbroken $I(q^*, T)$, contrary to the prediction of a first-order transition by both mean-field ($f \neq 1/2$) and fluctuation theory. None of these publications corroborate the assignment of T_{ODT} with rheological evidence of the phase transition.

Recently, Bates and co-workers (80) reported the preparation of fully saturated hydrocarbon diblock copolymers in the WSL. A series of monodisperse, $f \cong 0.55$, poly(ethylene-propylene)-poly(ethylethylene) (PEP-PEE) samples were studied rheologically (82) and by SANS (63, 81). Owing to the chemical similarity between blocks, this system exhibits an ODT at roughly five times the molecular weight of an equal composition polystyrene-polydiene material. For example, for $M_w = 57{,}400$ g/mole, Bates et al (63, 80–82) find $T_{ODT} \approx 100°C$. This higher molecular weight brings these polymers well into the rheologically entangled state at the ODT, which facilitates determining T_{ODT} (82). In principle, higher molecular weight polymers are also better candidates for evaluating the statistical mechanical WSL theories that are premised on a large N. Bates et al (63) have shown an exact correspondence between the temperature at which the rheological properties in a PEP-PEE sample are discontinuous and where $I(q^*)$ exhibits a subtle (20%) discontinuity. These results conclusively demonstrate the first-order character of the ODT and underscore the value of dynamic mechanical analysis in establishing T_{ODT}. However, contrary to Hashimoto et al (86, 87), Bates and co-workers (63) report $q^*(T)$ to be unaffected by the ODT.

A full evaluation of the PEP-PEE SANS results revealed the first clear evidence of composition fluctuations near the ODT. In the disordered state, the principle scattering reflection could be quantitativcly fit with the theoretical structure factor (Eq. 1). In addition, a shoulder was apparent at $q \cong 2q^*$ that became more prominent as the temperature was lowered towards T_{ODT}. This feature is not accounted for by current theory and suggests that the disordered phase may possess more "structure" (i.e. large composition gradients) than has previously been assumed. Overall, the disordered state SANS structure factor closely resembles the structure factor characterizing the final stage of spinodal-decomposition in a symmetric binary polymer mixture (99), which is the basis for the real-space morphology of the fluctuating disordered phase depicted in Figure 7. As shown in Figure 8, $I^{-1}(q^*)$ is clearly nonlinear in T^{-1} over the entire temperature range examined, which extends 56°C above T_{ODT}. A quantitative comparison of the mean-field and fluctuation theory predictions is also shown in Figure 8. [These calculations were made without adjustable parameters (63); N, f and $\chi(T)$ were determined independently (82).] This

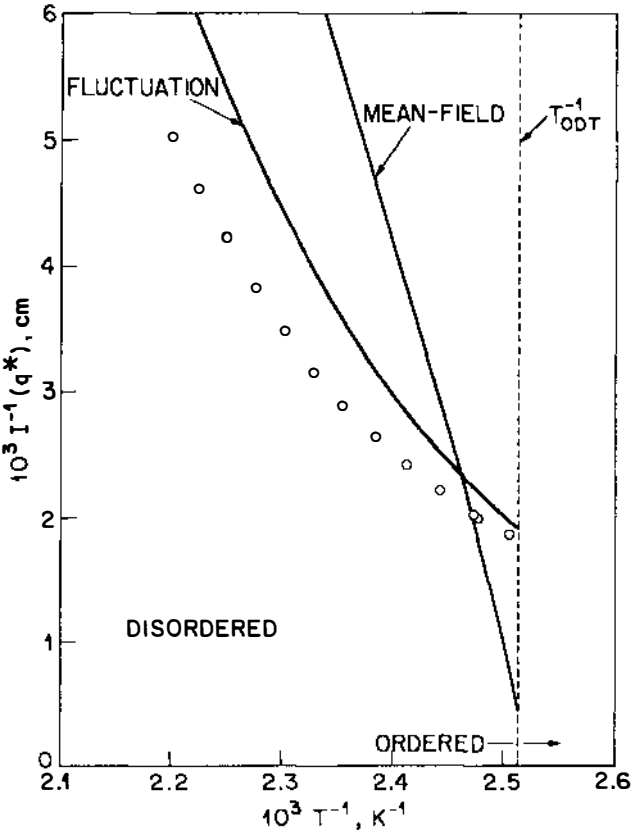

Figure 8 Reciprocal SANS peak intensity versus inverse temperature for a disordered model PEP-PEE diblock copolymer near T_{ODT}. The mean-field and fluctuation curves have been calculated (no adjustable parameters) by using the Landau (4) and fluctuation (62) theories, respectively, as described in Ref. (63).

comparison confirms the predicted significance of fluctuation effects in the disordered state near the ODT and rules out the use of a mean-field assumption in evaluating $I(q^*, T)$ in these regions of the block copolymer phase diagram.

Bates et al (63) also investigated the ordered state of a PEP-PEE specimen by using SANS. In order to facilitate these measurements, a sample was shear-oriented based on the principles established by Mathis et al (100). Scattering experiments revealed a lamellar morphology that persisted up to T_{ODT}, confirming the fluctuation theory prediction that for

slightly asymmetric compositions (here $f = 0.55$) the lamellar ordered phase should lead directly to the disordered phase (see Figure 6*b*); mean-field theory predicts a lamellar-hexagonal-(body-centered cubic)-disordered sequence of phase transitions (Figure 6*a*). Fluctuations were also evident in the two-dimensional SANS pattern (obtained from the oriented specimen) as the temperature approached T_{ODT}, in agreement with theory. Overall, the fluctuation theory is remarkably consistent with the (limited) experimental data (PEP-PEE, $f = 0.55$) available for comparison at the time of this writing, thus leading us to speculate that the real-space morphologies near the ODT resemble those depicted in Figure 7*b*; for $T \gg T_{ODT}$ and $T \ll T_{ODT}$ the classical pictures (Figure 7*a*) are recovered.

Near the ODT, the (polycrystalline) ordered and disordered states differ primarily in the extent of coherence of compositional order. Although this difference would be immediately apparent in direct images (see Figure 7*b*), the associated small-angle scattering patterns barely reflect the phase transition (63). Such long-range morphological features are best studied by direct methods such as transmission electron microscopy (TEM). Unfortunately, most model systems in the WSL are not readily studied by this technique. All the block copolymers considered in this review require staining prior to quantitative TEM analysis. Near the ODT, selective staining may seriously influence phase behavior, obviating use of the method. Samples that have chemically similar blocks such as PEP-PEE (80), are difficult if not impossible to stain selectively; a notable exception is the contrasting technique exploited by Cohen et al (76–78) in examining polydiene-polydiene block copolymers. Polystyrene-polydiene block copolymers are easily selectively stained and thus represent the most attractive candidates for TEM analysis (SSL-Experiment section). In fact, several provocative electron micrographs obtained from polystyrene-polyisoprene-polystyrene triblock copolymers quenched from near the ODT (T_{ODT} was well above the polystyrene glass transition temperature) to room temperature seem to exhibit disordered morphologies similar to that shown in Figure 7*b* (96, 101). The formation of a glassy component probably reduces the effects of stain-induced changes in miscibility. However, it is difficult to assess the impact of such large temperature changes above T_g on the nonequilibrium state of the sample. This method might be improved by placing T_{ODT} slightly above T_g for polystyrene, through adjustment of N, which would dramatically increase the system response time relative to the temperature quench time. Under such conditions, a quantitative analysis of demonstrably "frozen" structures could be conducted.

SURFACE BEHAVIOR

Experiment

Block copolymer surface properties have been a topic of great interest for several decades due in part to applications ranging from the formulation of adhesives to lubricating surfaces. Until recently, surface characterization tools have been limited to indirect methods such as X-ray photoelectron spectroscopy (XPS) and contact-angle wetting experiments. The past few years have witnessed vigorous growth in the area of surface analysis, particularly regarding block copolymer surfaces, due to the development of several new direct quantitative techniques, most notably dynamic secondary ion mass spectroscopy (SIMS), and neutron reflectometry.

Early investigations of the wetting properties of undiluted block copolymers, which dealt mainly with semicrystalline materials, indicated a significant degree of surface enrichment in one block component (102). This phenomenon was particularly evident in block copolymers containing polydimethylsiloxane, which exhibited low energy surfaces, consistent with the surface properties of polydimethylsiloxone homopolymer. Surface enrichment of polystyrene in polystyrene-poly(ethylene oxide) diblock copolymers was also quantified by Thomas & O'Malley (103) using XPS measurements. Recently, Green et al (104) have employed XPS to evaluate the surface properties of a series of polystyrene-polymethylmethacrylate diblock copolymers. They report a molecular weight dependent surface preference for polystyrene. Although these studies clearly demonstrate the existence of a preferred surface component, which is easily rationalized based on the pure component surface-tensions, the analytical methods discussed thus far are incapable of quantitatively delineating the actual surface profile or topology.

Direct evidence of surface segregation in a polystyrene-polyisoprene diblock copolymer was obtained with TEM by Hasegawa & Hashimoto (105). Solvent cast specimens were stained with osmium-tetraoxide, embedded in epoxy, and ultramicrotomed in preparation for microscopic examination. Regions of the ordered material (SSL) were photographed with lamellae arranged perpendicular and parallel to the free surface. In both cases, a thin polyisoprene layer, approximately half a bulk lamellar dimension thick, existed at the polymer surface. This technique is suitable for observing strongly segregated surfaces but is not likely to be effective in the weak segregation regime where staining could influence the system morphology.

SIMS is an alternative direct profiling technique that has recently been applied to the investigation of block copolymer surfaces. This method relies on the intensity of secondary ions (e.g. $^{1}H^{+}$, $^{2}H^{+}$, $^{12}C^{+}$, etc.) emitted as a function of time during primary ion beam sputtering of the surface. A

detailed SIMS analysis of a polystyrene-polymethyl methacrylate diblock copolymer film by Coulon et al (106) illustrated how effectively this method provides images of periodic lamellar structures that were formed parallel to the block copolymer free surface upon annealing at elevated temperatures. These authors estimate an instrument resolution of about 125 Å. Another popular ion beam technique that finds application in polymer surface studies, forward recoil spectroscopy (FRS), is generally not appropriate for block copolymer surface problems because of current resolution limitations ($\gtrsim$200 Å) (107).

The most recently developed surface analytical technique with direct applicability to block copolymers is neutron reflectometry. Here a collimated neutron beam produced by either a reactor or pulsed neutron source is directed at a sample surface and the reflected intensity is measured as a function of incident angle. Above the critical angle for total reflection ($\theta_c \approx 0.1°$), the reflected intensity is attenuated due to interference effects created by the sample composition profile, the free surface interface, and the substrate interface. By modeling the reflection curve, a detailed composition profile can be developed, with a high degree of sensitivity to both spatial dimensions ($\approx$2 Å resolution) and form. Russell and co-workers (83, 108, 109) have published a series of elegant neutron reflection studies conducted with as-cast and annealed polystyrene-polymethylmethacrylate diblock copolymers. A representative neutron reflection curve for an annealed specimen is shown in Figure 9. The solid curve in this illustration is the best-fit calculated reflectivity and corresponds to the composition profile shown in the inset. A slight variation in the composition profile (inset) produces significant changes in the calculated reflectivity as illustrated by the dashed curves. Russell and co-workers have exploited this powerful technique in examining a number of issues relating to surface segregation in thick and thin block copolymer films, including surface ordering and disordering as a function of temperature (109), and the quantitative evaluation of the interfacial profile in ordered lamellae (108). They report close agreement with mean-field theory (110) (see following section) for the surface induced formation of structure near the air-polymer interface, and a coincidence between the surface and bulk ODT temperature (109). Quantitative agreement with mean-field theory for these relatively low molecular weight specimens ($N \cong 300$) in the bulk state and at the surface is surprising given the strong fluctuation effects found in higher molecular weight PEP-PEE samples (63, 81, 82) (see Figure 8).

Theory

We are only aware of one theoretical study that has explicitly considered the behavior of block copolymer melts near a free surface or solid substrate.

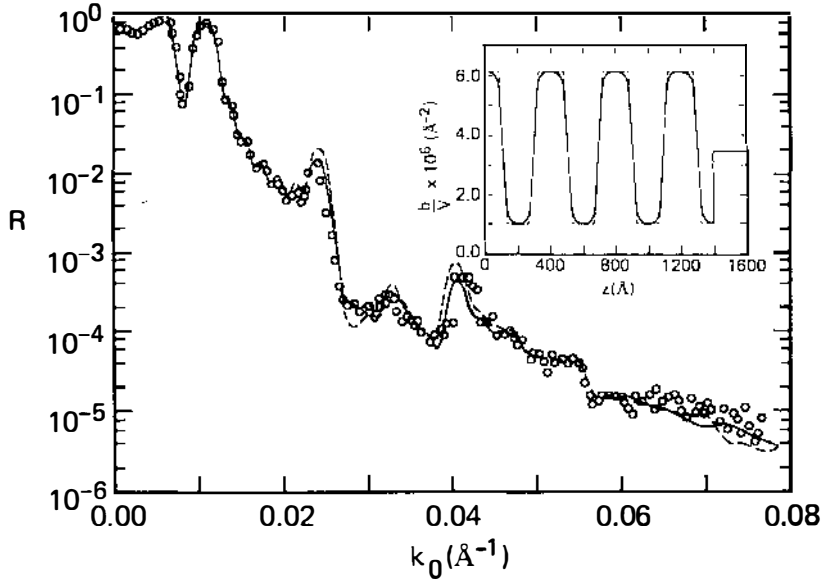

Figure 9 Neutron reflectivity R as a function of the neutron momentum transfer k_0 perpendicular to the surface of a thin annealed polydeuterostyrene-polymethylmethacrylate diblock copolymer film. The *solid* and *dashed curves* are the calculated reflectivities for the composition profiles shown in the *inset* (b/v is the neutron scattering length density) as reported in Ref. (108). (Provided by T. P. Russell.)

Fredrickson & Helfand (111) treated the case of a symmetric diblock copolymer melt in the WSL and in contact with such a surface. He employed a Landau approach, adding a surface free energy contribution to Leibler's bulk free energy expression (4). The surface term contained two phenomenological parameters H_1 and a_1 that describe the modifications of the (A–B exchange) chemical potential and the interaction parameter in the copolymer layer adjacent to the surface, respectively. By minimizing the sum of these bulk and surface free energy contributions with respect to variations in the composition field employed by Leibler, $\psi(\mathbf{r})$, Fredrickson derived an Euler-Lagrange equation for the composition pattern in the presence of a surface. At temperatures above the bulk ODT, $\chi N < (\chi N)_{ODT}$, any slight preference of monomer A or B for the surface, $|H_1| > 0$, proves sufficient to induce sinusoidal compositional order into the melt. The wavenumber of these oscillations is roughly equal to q^*, which characterizes the peak position in Leibler's diblock structure factor. Moreover, the oscillations are exponentially damped on the scale of

the disordered phase bulk correlation length, which is singular near the spinodal in Landau theory, $\xi_+ \sim R_g(1-\chi/\chi_s)^{-1/2}$. Similarly, below the bulk ODT, Fredrickson finds that the amplitude of the lamellar composition profile is modulated out to distances from the surface of order the correlation length, $\xi_- \sim R_g(\chi/\chi_s - 1)^{-1/2}$. Various surface phase transitions (110) are also possible for $H_1 = 0$, depending on the sign of a_1, although such conditions are likely very difficult to achieve in the laboratory.

In spite of the good agreement between the mean-field surface composition profile and the experiments of Russell and co-workers (83, 108, 109), we expect that extensions of the above theory to incorporate fluctuation effects will prove necessary. Extensions to treat systems with cylindrical, spherical, or OBDD bulk order would also be valuable.

DISCUSSION AND OUTLOOK

A survey of recent developments in block copolymer thermodynamics is presented in the previous sections. We have not attempted an exhaustive review of this expansive subject. Instead, we have restricted our attention to studies dealing with fundamental issues pertaining to order and disorder in this complex and fascinating class of materials. Recent theoretical advances in this area relate exclusively to model $(A–B)_n$ type materials; for the most advanced studies involving fluctuation effects, the focus narrows to A–B diblock and triblock copolymers. In considering a vast experimental literature we have opted to limit our scope to selected publications relevant to current theory, or those likely to provoke new theoretical efforts. Despite these restrictions, there still exist a number of significant deficiencies in our understanding of this field.

At present there is no theory capable of predicting the existence of the ordered bicontinuous double diamond phase in the strong segregation limit. In addition, there is no experimental or theoretical evidence to prove or disprove that the OBDD phase can be accessed at the ODT. However, the beautiful morphological studies of Thomas and co-workers, and the connections that they have made to the mathematical science of minimal surfaces, should provide new impetus for exploring fresh approaches to the above problems.

In our opinion the major unresolved issues in block copolymer thermodynamics are associated with the order-disorder transition, which we have included under the heading of weak segregation limit. Foremost amongst these problems is the notion of the WSL itself. The WSL assumption originated with Leibler's mean-field treatment (4), and was retained by

Fredrickson & Helfand (62) when fluctuation effects were incorporated into the theory. Our binary classification scheme of WSL and SSL remains a convenient and obvious one when dealing with currently available theories. However, categorizing the experimental studies near the ODT under these two headings is not so straightforward. Clearly there exist limits at sufficiently large and small values of χN at which block copolymers conform to the SSL and WSL assumptions. Nevertheless it must be recognized that at present there is no theoretical estimate of the size or location of the intermediate region between these limiting behaviors. WSL theories assume a sinusoidal composition profile in the ordered phase, and unperturbed Gaussian coil behavior. Whether this accurately reflects the true situation in the transition region is simply unknown. An important challenge for theorists is to develop a comprehensive theory that deals with the crossover from the WSL to the SSL.

Although recent SANS experiments (63, 81) support the qualitative (and to some extent, quantitative) predictions regarding composition fluctuations near the ODT, several troubling inconsistencies challenge the underlying WSL assumption. The observation of a shoulder at approximately twice the principle SANS reflection at temperatures above T_{ODT} by Bates et al (63) cannot be explained by the perturbative methods implicit in the WSL theories. In fact, similarities between the disordered state structure factor and the final stage spinodal decomposition scattering pattern suggests a rather strongly segregated, albeit disordered, state. This recent finding is reminiscent of the SAXS results reported by Roe et al (25) nearly a decade ago, in which narrow ($\approx$20 Å) interfacial thicknesses were determined above T_{ODT}. Stronger than predicted segregation in the disordered state might also account for the anomalous low frequency rheological response found near the ODT (82, 92, 111). Off-symmetry SANS measurements also suggest the existence of "domain-like" entities within the disordered melt (56), which have been predicted by Semenov (65) in the limit of small (or large) f.

These experimental findings near the order-disorder transition raise serious questions concerning the weak segregation limit assumption, and may invalidate our classification scheme. We believe that the resolution of this issue will require both new theoretical approaches and additional quantitative experiments.

Finally, we have included block copolymer surfaces in this review. Only very recently have quantitative experimental techniques (e.g. SIMS and neutron reflectometry) been introduced in this field. Although identifying subjects that hold unusual promise is risky, we feel quite certain that developments in this area will come rapidly, and will have wide scientific and technological impact.

ACKNOWLEDGMENTS

We are indebted to our collaborators E. Helfand, R. Larson, L. Leibler, and J. Rosedale for their contributions to our understanding of the issues covered in this review. F.S.B. also acknowledges support from the NSF under PYI Grant DMR-8957386.

Literature Cited

1. Szwarc, M., Levy, M., Milkovich, R. 1956. *J. Am. Chem. Soc.* 78: 2656
2. Schlick, S., Levy, M. 1960. *J. Phys. Chem.* 64: 883
3. deGennes, P. G. 1979. *Scaling Concepts in Polymer Physics.* Ithaca: Cornell Univ. Press
4. Leibler, L. 1980. *Macromolecules* 13: 1602
5. Helfand, E., Wasserman, Z. R. 1982. See Ref. 7, p. 99
6. Semenov, A. N. 1985. *Soviet Phys. JETP* 61: 733
7. Goodman, I., ed. 1982. *Developments in Block Copolymers—1.* New York: Applied Sci.
8. Goodman, I., ed. 1985. *Developments in Block Copolymers—2.* New York: Applied Sci.
9. Meier, D. J., ed. 1983. *Block Copolymers: Science and Technology.* New York: MMI Press/Harwood Academic Publ.
10. Allport, D. C., Jones, W. H., eds. 1973. *Block Copolymers.* New York: Wiley
11. Aggarwal, S. L., ed. 1970. *Block Copolymers.* New York: Plenum
12. Burke, J. J., Weiss, V., eds. 1973. *Block and Graft Copolymers.* New York: Syracuse Univ. Press
13. Hashimoto, T., Nagatoshi, K., Todo, A., Hasegawa, H., Kawai, H. 1974. *Macromolecules* 7: 364
14. Hashimoto, T., Todo, A., Itoi, H., Kawai, H. 1977. *Macromolecules* 10: 377
15. Todo, A., Uno, H., Miyoshi, K., Hashimoto, T., Kawai, H. 1977. *Polym. Eng. Sci.* 17: 527
16. Hashimoto, T., Shibayama, M., Kawai, H. 1980. *Macromolecules* 13: 1237
17. Hashimoto, T., Fujimura, M., Kawai, H. 1980. *Macromolecules* 13: 1660
18. Fujimura, M., Hashimoto, H., Kurahashi, K., Hashimoto, T., Kawai, H. 1981. *Macromolecules* 14: 1196
19. Ruland, W. 1971. *J. Appl. Crystallogr.* 4: 70
20. Vonk, C. G. 1973. *J. Appl. Crystallogr.* 6: 81
21. Koberstein, J., Morra, B., Stein, R. S. 1980. *J. Appl. Crystallogr.* 13: 34
22. Bates, F. S., Berney, C. V., Cohen, R. E. 1983. *Macromolecules* 16: 1101
23. Bates, F. S., Cohen, R. E., Berney, C. V. 1982. *Macromolecules* 15: 584
24. Richards, R. W., Thomason, J. L. 1983. *Macromolecules* 16: 982
25. Roe, R. J., Fishkis, M., Chang, J. C. 1981. *Macromolecules* 14: 1091
26. Spontak, R. J., Williams, M. C., Agard, D. A. 1988. *Macromolecules* 21: 1377
27. Aggarwal, S. L. 1976. *Polymer* 17: 938
28. Alward, D. B., Kinning, D. J., Thomas, E. L., Fetters, L. J. 1986. *Macromolecules* 19: 215
29. Kinning, D. J., Alward, D. B., Thomas, E. L., Fetters, L. J., Handlin, D. J. 1986. *Macromolecules* 19: 1288
30. Fetters, L. J. 1983. See Ref. 9, p. 17
31. Thomas, E. L., Alward, D. B., Kinning, D. J., Handlin, D. L., Fetters, L. J. 1986. *Macromolecules* 19: 2197
32. Hasegawa, H., Tanaka, H., Yamasaki, K., Hashimoto, T. 1987. *Macromolecules* 20: 1651
33. Herman, D. S., Kinning, D. J., Thomas, E. L., Fetters, L. J. 1987. *Macromolecules* 20: 2940
34. Thomas, E. L., Anderson, D. M., Henkee, C. S., Hoffman, D. 1988. *Nature* 334: 598
35. Richards, R. W., Thomason, J. L. 1981. *Polymer* 22: 581
36. Hadziioannou, G., Picot, C., Skoulios, A., Ionescu, M.-L., Mathis, A., et al. 1982. *Macromolecules* 15: 263
37. Jahshan, S. N., Summerfield, G. C. 1980. *J. Polym. Sci. Polym. Phys. Ed.* 20: 593
38. Koberstein, J. T. 1982. *J. Polym. Sci. Polym. Phys. Ed.* 20: 593
39. Bates, F. S., Berney, C. V., Cohen, R. E., Wignall, G. D. 1983. *Polymer* 24: 519
40. Hasegawa, H., Hashimoto, T., Kawai, H., Lodge, T. P., Amis, E. J., et al. 1985. *Macromolecules* 18: 67
41. Hasegawa, H., Tanaka, H., Hashi-

moto, T., Han, C. C. 1987. *Macromolecules* 20: 2120
42. Matsushita, Y., Nakao, Y., Saguchi, R., Mori, K., Choshi, H., et al. 1988. *Macromolecules* 21: 1802
43. Meier, D. J. 1969. *J. Polym. Sci. C* 26: 81
44. Leary, D. F., Williams, M. C. 1970. *J. Polym. Sci. B* 8: 335
45a. Helfand, E. 1975. *Macromolecules* 8: 552
45b. Helfand, E., Wasserman, Z. R. 1976. *Macromolecules* 9: 879
46. Milner, S. T., Witten, T. A., Cates, M. E. 1988. *Europhys. Lett.* 5: 413; 1988. *Macromolecules* 21: 2610
47a. Milner, S. T., Witten, T. A., Cates, M. E. 1988. *Macromolecules* 22: 853
47b. Milner, S. T., Witten, T. A. 1988. *J. Phys. Paris* 19: 1951
48a. Ohta, T., Kawasaki, K. 1986. *Macromolecules* 19: 2621
48b. Kawasaki, K., Ohta, T., Kohrogui, M. 1988. *Macromolecules* 21: 2972
49. Anderson, D. M., Thomas, E. L. 1988. *Macromolecules* 21: 3221
50. Toledano, J.-C., Toledano, P. 1987. *The Landau Theory of Phase Transitions.* Teaneck, NJ: World Scientific
51. de Gennes, P. G. 1979. *Faraday Discuss. Chem. Soc.* 68: 96
52. LeGrand, A. D., LeGrand, D. G. 1979. *Macromolecules* 12: 450
53. de la Cruz, M. O., Sanchez, I. C. 1986. *Macromolecules* 19: 2501
54. Benoit, H., Hadziioannou, G. 1988. *Macromolecules* 21: 1449
55. Leibler, L., Benoit, H. 1981. *Polymer* 22: 195
56. Bates, F. S., Hartney, M. A. 1985. *Macromolecules* 18: 2478; 1986. *Macromolecules* 19: 2892
57. Benoit, H., Wu, W., Benmouna, M., Mozer, B., Bauer, B., Lapp, A. 1985. *Macromolecules* 18: 986; Ionescu, L., Picot, C., Duval, M., Duplessix, R., Benoit, H. 1981. *J. Polym. Sci. Polym. Phys. Ed.* 19: 1019
58. Mori, K., Tanaka, H., Hasegawa, H., Hashimoto, T. 1989. *Polymer* 30: 1389
59. Ma, S. K. 1976. *Modern Theory of Critical Phenomena.* Reading, Mass.: Benjamin-Cummings
60. Brazovskii, S. A. 1975. *Soviet Phys. JETP* 41: 85
61. Binder, K. 1987. *Rep. Prog. Phys.* 50: 783
62. Fredrickson, G. H., Helfand, E. 1987. *J. Chem. Phys.* 87: 697
63. Bates, F. S., Rosedale, J. H., Fredrickson, G. H. 1990. *J. Chem. Phys.* 92: 6255
64. Gunton, J. D., San Miguel, M., Sahni, P. S. 1983. *Phase Transitions and Critical Phenomena,* ed. C. Domb, J. L. Lebowitz, 8: 267. New York: Academic
65. Semenov, A. N. 1989. *Macromolecules* 22: 2849
66. Mayes, A. M., Olvera de la Cruz, M. 1989. *J. Chem. Phys.* 91: 7228
67. Fredrickson, G. H., Leibler, L. 1989. *Macromolecules* 22: 1238
68. de la Cruz, M. O. 1989. *J. Chem. Phys.* 90: 1995
69. Hashimoto, T., Shibayama, M., Kawai, H. 1983. *Macromolecules* 16: 1093; 1427; 1434
70. Hong, K. M., Noolandi, J. 1983. *Macromolecules* 16: 1083
71. Baer, M. 1964. *J. Polymer Sci. A* 2: 417
72. Robeson, L. M., Matzner, M., Fetters, L. J., McGrath, J. E. 1974. *Recent Advances in Polymer Blends, Grafts and Blocks,* ed. L. H. Sperling, p. 281. New York: Plenum
73. Krause, S., Dunn, D. J., Seyed-Mozzaffari, A., Biswas, A. M. 1977. *Macromolecules* 10: 786
74. Mori, K., Hasegawa, H., Hashimoto, T. 1985. *Polym. J.* 17: 799
75. Owens, J. N., Gancarz, I. S., Koberstein, J. T., Russell, T. P. 1989. *Macromolecules* 22: 3380
76. Ramos, A. R., Cohen, R. E. 1977. *Polym. Eng. Sci.* 17: 639
77. Cohen, R. E., Ramos, A. R. 1979. *Macromolecules* 12: 131
78. Cohen, R. E., Wilfong, D. E. 1982. *Macromolecules* 15: 370
79. Fischer., E. W., Jung, W. G. 1989. *Makromol. Chem. Macromol. Symp.* 26: 179; 16: 281
80. Bates, F. S., Rosedale, J. H., Bair, H. E., Russell, T. P. 1989. *Macromolecules* 22: 2557
81. Bates, F. S., Rosedale, J. H., Fredrickson, G. H., Glinka, C. J. 1988. *Phys. Rev. Lett.* 61: 2229
82. Rosedale, J. H., Bates, F. S. 1990. *Macromolecules* 23: 2329
83. Anastasiadis, S. H., Russell, T. P., Satija, S. K., Majkrzak, C. F. 1989. *Phys. Rev. Lett.* 62: 1852
84. Green, P. F., Russell, T. P., Jerome, R., Granville, M. 1988. *Macromolecules* 21: 3266
85. Fetters, L. J., Richards, R. W., Thomas, E. L. 1987. *Polymer* 18: 2252
86. Hashimoto, T., Ijichi, Y., Fetters, L. J. 1988. *J. Chem. Phys.* 89: 2463
87. Ijichi, Y., Hashimoto, T., Fetters L. J. 1989. *Macromolecules* 22: 2817
88. Bates, F. S., Bair, H. E., Hartney, M. A. 1984. *Macromolecules* 17: 1987
89a. Chung, C. I., Gale, J. C. 1976. *J. Polym. Sci. Polym. Phys. Ed.* 14: 1149

89b. Chung, C. I., Lin, M. I. 1978. *J. Polym. Sci. Polym. Phys. Ed.* 16: 545
90. Pico, E. R., Williams, M. C. 1976. *Nature* 259: 388
91. Ferry, J. D. 1980. *Viscoelastic Properties of Polymers*. New York: Wiley. 3rd ed.
92. Bates, F. S. 1984. *Macromolecules* 17: 2607
93. Han, C. D., Kim, J., Kim, J. K. 1987. *J. Polym. Sci. Polym. Phys. Ed.* 25: 1741
94. Han, C. D., Kim, J., Kim, J. K. 1989. *Macromolecules* 22: 383
95. Han, C. D., Balk, D. M., Kim, J. K. 1990. Preprint
96. Widmaier, J. J., Meyer, G. C. 1980. *J. Polym. Sci. Polym. Phys. Ed.* 18: 2217
97. Gouinlock, E. V., Porter, R. S. 1977. *Polym. Eng. Sci.* 17: 535
98. Bates, F. S. 1985. *Macromolecules* 18: 525
99. Bates, F. S., Wiltzius, P. 1989. *J. Chem. Phys.* 91: 3258
100. Mathis, A., Hadziioannou, G., Skoulios, A. 1977. *Polym. Eng. Sci.* 17: 570; 1979. *Colloid Polym. Sci.* 257: 136
101. Hadziioannou, G., Skoulios, A. 1982. *Macromolecules* 15: 258
102. Owen, M. J. 1983. See Ref. 9, p. 129
103. Thomas, H. R., O'Malley, J. J. 1979. *Macromolecules* 12: 323
104. Green, P. F., Christensen, T. M., Russell, T. P., Jerome, R. 1989. *Macromolecules* 22: 2189
105. Hasegawa, H., Hashimoto, T. 1985. *Macromolecules* 18: 589
106. Coulon, G., Russell, T. P., Deline, V. R., Green, P. F. 1989. *Macromolecules* 22: 2581
107. Chaturvedi, U. K., Steiner, U., Zak, O., Krausch, G., Klein, J. 1989. *Phys. Rev. Lett.* 63: 616
108. Anastasiadis, S. H., Russell, T. P., Satija, S. K., Majkrzak, C. F. 1990. *J. Chem. Phys.* 92: 5677
109. Russell, T. P., Anastasiadis, S. H., Satija, S. K., Majkrzak, C. F. 1990. To be submitted
110. Fredrickson, G. H. 1987. *Macromolecules* 10: 2535
111. Fredrickson, G. H., Helfand, E. 1988. *J. Chem. Phys.* 89: 5890